Chemical Science

EDGE ARTICLE

View Article Online
View Journal | View Issue

Cite this: *Chem. Sci.*, 2016, **7**, 4418

Stable end-sealed DNA as robust nano-rulers for *in vivo* single-molecule fluorescence†

A. Plochowietz,*[a] A. H. El-Sagheer,[bc] T. Brown[b] and A. N. Kapanidis*[a]

Single-molecule fluorescence and Förster resonance energy transfer (smFRET) are important tools for studying molecular heterogeneity, cellular organization, and protein structure in living cells. However, *in vivo* smFRET studies are still very challenging, and a standardized approach for robust *in vivo* smFRET measurements is still missing. Here, we synthesized protected DNAs with chemically linked ends as robust *in vivo* nano-rulers. We efficiently internalized doubly-labeled end-sealed DNA standards into live bacteria using electroporation and obtained stable and long-lasting smFRET signatures. Single-molecule fluorescence signals could be extended to ~1 min by studying multi-fluorophore DNA standards. The high stability of protected DNA standards offers a general approach to evaluate single-molecule fluorescence and FRET signals, autofluorescence background, and fluorophore density, and hence, quality check the workflow for studying single-molecule trajectories and conformational dynamics of biomolecules *in vivo*.

Received 10th February 2016
Accepted 21st March 2016

DOI: 10.1039/c6sc00639f

www.rsc.org/chemicalscience

Introduction

Single-molecule fluorescence and single-molecule Förster resonance energy transfer (smFRET) studies have advanced substantially our understanding of molecular and cellular processes over the last two decades.[1–3] Single-molecule fluorescence is increasingly employed *in vivo* to study gene expression stochasticity and spatial organization of biomolecules in the natural cellular environment, whereas smFRET is well suited for studying protein structure and dynamics both *in vitro* and in living cells.[4,5] FRET relies on the non-radiative energy transfer from a donor fluorophore (D) to a complementary acceptor fluorophore (A) present in close proximity (2–10 nm).[6–8] *In vitro* smFRET has been used extensively to study many processes including nucleic acid and protein folding,[9,10] and conformational changes of large protein complexes;[11–15] these studies enabled structure-function single-molecule analysis and uncovered mechanistically relevant molecular heterogeneities.

Despite the extensive use of smFRET *in vitro*, live-cell smFRET studies are still challenging, mainly due to the difficulty of site-specific FRET dye-pair labeling of biomolecules in living cells.[16] Fluorescent proteins (FPs) are often employed as *in vivo* FRET dye-pairs, but their photophysical properties (blinking, poor photostability, low brightness) prevent their use in single-molecule FRET studies.[17,18] Further, labeling strategies using FPs (~100-fold larger than organic dyes) are limited to protein end-labeling.[5]

In contrast, organic dyes are much better suited for smFRET; however, they have to be introduced into live cells by *in vivo* specific protein labeling *via* polypeptide tags (SNAP, HALO, or TMP tags[19–21]) or *via* unnatural amino acids;[22] alternatively, delivery can rely on internalization of *in vitro* organic-dye labeled proteins into live cells. The latter strategy was used in a handful of smFRET studies in live prokaryotic[23] and eukaryotic[24,25] cells. In one of these approaches, we used electroporation to internalize doubly-labeled DNAs and DNA-binding proteins into live bacteria[23,26] and characterized organic dyes for their use in *in vivo* FRET studies.[27]

To characterize *in vivo* FRET measurements, we previously used blunt-ended 45-bp double-stranded DNA with different donor–acceptor distances to monitor low-, intermediate-, and high-FRET signals inside single cells. In those studies, we observed decreased FRET for some of the internalized DNA compared to *in vitro* measurements,[23,27] and attributed this shift mainly to *in vivo* DNA degradation by endonucleases that recognize blunt DNA ends and digest DNA.[28]

The absence of robust DNA standards that report on FRET, degradation processes, and cellular autofluorescence has slowed down the implementation of single-molecule fluorescence and FRET studies in living cells. Here, we address this limitation by introducing doubly-labeled protected DNA FRET standards and multi-fluorophore protected DNAs, in which both DNA ends are chemically linked using click chemistry

[a]*Department of Physics, University of Oxford, Clarendon Laboratory, Parks Road, Oxford, OX1 3PU, UK. E-mail: anne.plochowietz@gmail.com; a.kapanidis1@physics.ox.ac.uk*

[b]*Department of Chemistry, University of Oxford, Chemistry Research Laboratory, 12 Mansfield Road, Oxford, OX1 3TA, UK*

[c]*Chemistry Branch, Department of Chemistry, Faculty of Petroleum and Mining Engineering, Suez University, Suez 43721, Egypt*

† Electronic supplementary information (ESI) available: Experimental methods, data analysis routines and Fig. S1–S9. See DOI: 10.1039/c6sc00639f

(Scheme 1, ESI†) to prevent DNA degradation inside live *E. coli*. The protection of oligonucleotide termini was previously demonstrated for cyclic dumbbell DNA duplexes.[29,30] Here, the CuAAC reaction was chosen for three reasons: (i) its high efficiency in aqueous media, (ii) its orthogonality with the functional groups of DNA and the primary amino groups used as attachment points for fluorescent dyes, and (iii) the simplicity of introducing the alkyne and azide functions into oligonucleotide strands.

Results

Our protected DNA FRET standards were initially characterized *in vitro* and internalized into live *E. coli* using electroporation. We employed alternating laser excitation (ALEX, ref. 31 and 32) *in vivo* to identify donor–acceptor molecules and show that their FRET values agree very well with our *in vitro* measurements. We also combined smFRET measurements with single-particle tracking and obtained stable and long-lasting smFRET trajectories (~10 s), and multi-fluorophore DNA trajectories (~1 min), showing that the protected DNAs are well suited to monitor smFRET levels in living cells.

We synthesized doubly-labeled 45-bp protected DNAs with different dye spacing corresponding to intermediate-FRET efficiencies (18 bp spacing, hereafter P18), and high-FRET efficiencies (8 bp spacing, hereafter P8; Scheme 1, ESI†). We used the FRET pair Cy3B/Atto647N, which we previously showed to perform well in single-cell FRET studies.[27]

To characterize the stability of the protected DNA FRET standards *in vitro* and test for any effects of their exposure to electroporation conditions (as tested in the electroporation cuvette but in the absence of cells), we used confocal ALEX microscopy (Experimental section). Both the fluorescence intensity time-traces and their autocorrelation function of electroporated protected DNAs (ACF; ESI†) showed the typical burst duration (~1–2 ms) expected

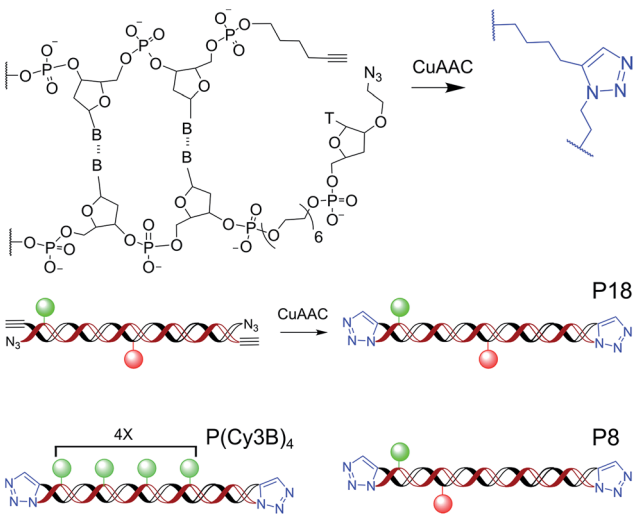

Scheme 1 Templated click ligation to synthesize end-sealed DNA duplexes; fluorophores are shown for intermediate-FRET (P18), high-FRET (P8), and multi-fluorophore DNA standards $(P(Cy3B)_4)$.

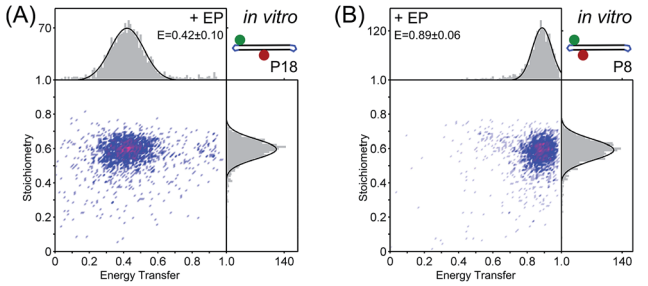

Fig. 1 *In vitro* characterization of (A) protected intermediate-FRET DNA (P18) and (B) protected high-FRET DNA (P8) using confocal ALEX microscopy. FRET-stoichiometry histograms show single intermediate- and high-FRET species after electroporation with single Gaussian fits centered at $E = 0.42 \pm 0.10$ and $E = 0.89 \pm 0.06$ (±standard deviation), respectively. E values are corrected for cross-talk contributions and different detector efficiencies at each emission channel,[32] see ESI and Fig. S5.†

for a DNA of their size, and indicated the presence of a single diffusing species both before and after electroporation (Fig. S1†). This was in contrast to unprotected, blunt-ended DNA FRET standards, for which DNA aggregated during electroporation (Fig. S2;† 20–30 ms burst length); this aggregation was overcome by adding 1 mM EDTA to blunt-ended DNAs before electroporation (Fig. S2†), likely due to EDTA chelating Al^{3+}-ions released from the electroporation cuvette.[33]

Sorting the fluorescence bursts in 2D-histograms of FRET (E) and probe stoichiometry (S, a fluorescence ratio that reports on molecular stoichiometry, ESI†), we observed a single FRET species both for electroporated P18 ($E \sim 0.42$) and electroporated P8 ($E \sim 0.89$) (Fig. 1). The excellent agreement of ES-histograms for the FRET standards before and after electroporation for six different electroporation voltages (0.8–1.8 kV, Fig. S3†), as well as the absence of free dye[26] (Fig. S4†) make the protected DNAs well suited for internalization into live bacteria. FRET and stoichiometry values were corrected for cross-talk contribution and different detector efficiencies at each emission channel (γ-factor). Technical detail are given in the ESI,† the contribution of the different correction terms to the ES-histograms for *in vitro* measurements are shown in Fig. S5,† and the estimation of the γ-factor is shown in Fig. S6.†

To evaluate the performance of the protected DNA standards *in vivo*, we electroporated them into live *E. coli*, recovered electroporated cells, and removed non-internalized DNAs by washing before imaging (Experimental section). We applied an initial electric field of 14 kV cm^{-1}, which maintained ~70% cell viability[27] and resulted in a cellular uptake of up to 8 DNA molecules per cell (median: ~1 molecule per cell). We imaged cells on agarose pads by an inverted wide-field fluorescence microscope using HILO illumination[34] combined with ALEX (Experimental section).

We sorted species (Fig. 2A) into FRET molecules (which contain both an emitting donor and an emitting acceptor), donor-only molecules, and acceptor-only molecules. Single-molecule localization of FRET molecules was first performed using the FRET channel (*i.e.*, donor-excitation/acceptor emission channel; DA

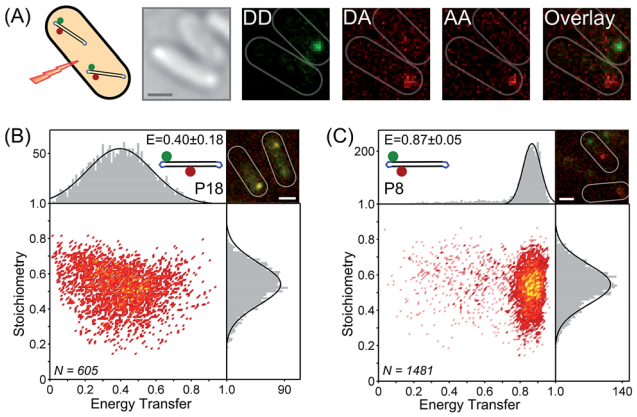

Fig. 2 *In vivo* characterization of protected DNA FRET standards. (A) Electroporation of protected high FRET DNA standards into live *E. coli* and observation of smFRET signals using an alternating laser excitation scheme (ALEX) monitoring D-only (DD channel), A-only (AA channel), and smFRET (DA channel) molecules. (B–C) Accurate FRET-stoichiometry histograms of P18 and P8 standards; the main FRET species are centered at $E = 0.40 \pm 0.18$ and at $E = 0.87 \pm 0.05$, respectively. *N* denotes the number of selected molecules P18: ~45%, and P8: ~30% of all initial localizations, 3 independent data sets are combined (~1000 cells each, 0–2 FRET molecules per cell) and example cell images are shown as a composite of DD- and DA-channel (overlay) such that high-FRET, intermediate-FRET, and D-only DNA molecules appear red, yellow, and green, respectively.

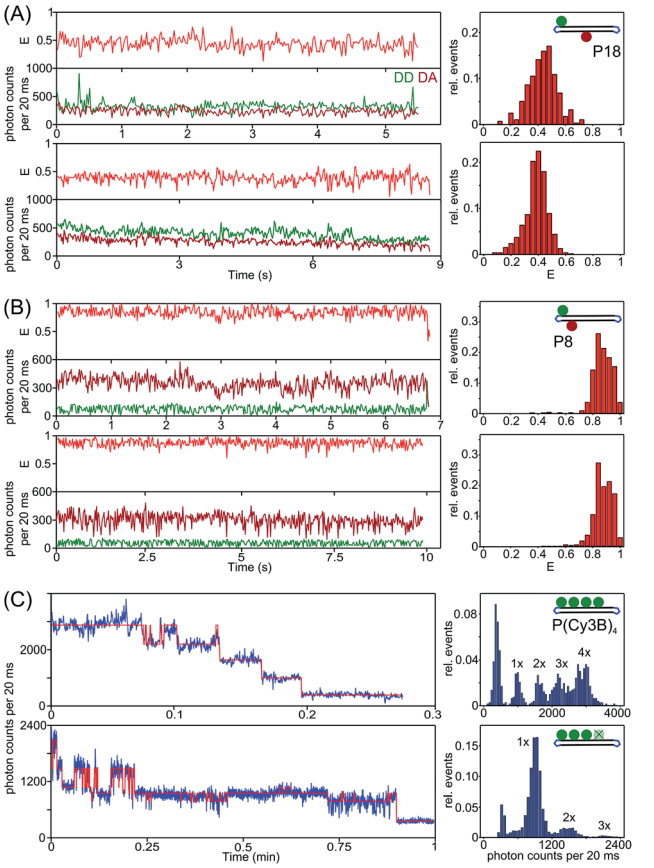

Fig. 3 Long-lasting observation of protected DNA standards using single-particle tracking. (A–B) Accurate smFRET time-traces and FRET-histograms showing *E*-values (red), DD-intensity (dark green), and DA-intensity (dark red) of single protected intermediate and high DNA FRET molecules, respectively. These FRET time-traces showed anti-correlated DD and DA-signals, a hallmark of single-molecule FRET (*e.g.* B: top time-trace) and spikes in DD-signal due to nearby D-only molecules (*e.g.* A: top time-trace). More smFRET showing donor and acceptor photobleaching events are shown in Fig. S9.† (C) Single-molecule fluorescence time-traces of multi-fluorophore protected DNA showing distinct photobleaching events and fluorophore blinking (blue: raw data, red: HMM fit, ESI†). Single-molecule intensity histograms show 3–4 Cy3B-labels per single DNA molecule.

channel), where there is little interference from donor-only, acceptor-only species, and autofluorescence; we then mapped the DA signal to the corresponding signal in the donor-excitation/donor emission channel (DD channel), and linked these signals to the acceptor-excitation/acceptor emission channel (AA channel; ESI†). We only included molecules with >400 photons per frame (for DD + DA) above the cellular autofluorescence to ensure accurate fitting of single molecule images in the respective channels (Fig. S7, ESI†); the 2D Gaussian fitting of the images accounted for the different cellular autofluorescence in the respective fluorescence channels.

The ES histograms for the selected species were also corrected for cross-talk and γ-factor contributions (Fig. S8†) and showed a single FRET species for P18 ($E = 0.40 \pm 0.18$; Fig. 2B), and for P8 ($E = 0.87 \pm 0.05$; Fig. 2C). The mean FRET efficiencies obtained *in vivo* were in excellent agreement with *in vitro* FRET values (0.42 and 0.89, respectively) and did not show a shift towards smaller FRET values as previously seen for immobile blunt-ended DNA.[23] The increased width of the fitted Gaussian distribution was due to the *in vivo* smFRET signals being noisier than *in vitro* signals, which we mainly attribute to effects of molecular motion, cellular autofluorescence, and nearby molecules.

To test our ability to perform extended observations using protected DNAs, we tracked single FRET molecules in single cells while monitoring their FRET signatures in green continuous-wave mode (ESI†). We tracked smFRET molecules for >10 s and obtained stable and long-lasting smFRET time-traces (Fig. 3A and B). The time-traces show different levels of noise due to molecular motion and cellular autofluorescence. The smFRET observation time is mainly limited by photobleaching, but can be extended to the min-timescale using time-lapse imaging.

To extend the single-molecule fluorescence observation of internalized DNAs, we also studied a protected multi-fluorophore DNA standard labeled with 4 Cy3B fluorophores ($P(Cy3B)_4$, Scheme 1). Long-lasting (>10 s) single-molecule fluorescence time-traces were picked and Hidden Markov Modeling analysis was applied to elucidate single photobleaching and blinking events. We observed up to 4 distinct photobleaching steps and fluorescence signal from a single DNA molecule for >50 s (Fig. 3C). The fluorescence intensity per Cy3B fluorophore was estimated to ~30 000 photons per s, which could increase the temporal resolution by 2–3 fold, and extend single-molecule observation to a few minutes.

Conclusions

Our results establish that protected DNAs can serve as excellent standards for *in vivo* single-molecule fluorescence due their efficient internalization into *E. coli* and their long-lived stability. Interestingly, our results show that the cellular environment does not dramatically affect the fluorophore properties (at least when fluorophores are photoactive) and corrected FRET efficiencies of the standards (no significant DNA degradation), and that *in vitro* and *in vivo* smFRET efficiencies agreed remarkably well, despite being acquired in different media (cellular cytoplasm *vs.* an aqueous buffer). In addition, we were able to obtain stable smFRET time-traces for ~10 s and long-lasting multi-fluorophore single-molecule fluorescence time-traces of >50 s in the bacterial cytoplasm. These results make the protected DNA standards ideal for robust single-molecule fluorescence observation and help to implement smFRET in living cells.

The *in vivo* use of DNA standards can be further improved. Due to the wide range of internalized molecules per cell (0–8, median: 1 molecule per cell), single-particle tracking was impeded by nearby molecules (ideally: ~1–3 molecules per cell, 1 mol μm^{-2}, ref. 35). This "crowding" scenario, along with higher autofluorescence (especially in the DD channel) also skewed smFRET signals (*e.g.*, due to DD-signal spikes, Fig. 3A), since the single-molecule localization routine relies on assuming that only a single fluorophore contributes to the fluorescence signal. Thus, performing smFRET in the 650–800 nm range (*e.g.* using Cy5/Cy7, and Atto680/Atto740, ref. 18), where autofluorescence is minimized, will offer a "cleaner" spectral window for smFRET.

The protected DNAs should be used as reference "nanorulers" to calibrate and check the quality of *in vivo* smFRET measurements, report on cellular autofluorescence background, and help optimize the fluorophore density for single-molecule observation in living cells. The stable end-sealed DNAs are versatile and can easily be modified to become standards for co-localization studies, multi-color experiments beyond FRET, or reporters on complex stoichiometries such as the $P(Cy3B)_4$ standard. Finally, protected DNA substrates with modified functional groups and varying DNA sequences could be employed to study specific DNA–protein interactions and their spatial distribution within the living cell. These dsDNA can act as 'decoys' (*e.g.* copies of transcription factor sites) and effectively compete with chromosomal sites and alter gene expression.

Experimental

DNA sequences are shown 5′ to 3′:

S1: TAAATCTAAAGTAACATAAGGTAACATAACGTAAGCTCAT TCGCG

S2: CGCGAATGAGCTTACGTTATGTTACCTTATGTTACTTTA GATTTA

S3: CGCGAATGAGCTTACGTTATGTTACCTTATGTTACTTTA GATTTA

S4: TAAATCTAAAGTAACATAAGGTAACATAACGTAAGCTCAT TCGCG

S5: CGCGAATGAGCTTACGTTATGTTACCTTATGTTACTTTA GATTTA

The highlighted T base was labeled with Cy3B (GE Healthcare) for strand S1 and S4, and with Atto647N (ATTO-TEC GmbH) for strand S2 and S3. Protected high FRET DNA standard: S1/S2, protected intermediated FRET DNA standard: S1/S3, and multi-fluorophore DNA standard: S4/S5 were chemically linked using azide–alkyne click-chemistry (Scheme 1). Experimental details and chemical structures of DNA modifications are shown in the ESI.† Protected DNA FRET standards were stored in ddH_2O at −20 °C.

In vitro single-molecule FRET measurements and fluorescence correlation spectroscopy (FCS) measurements were performed on a custom-built confocal microscope.[36] The confocal setup consisted of two laser lines, a 638 nm diode laser (Cube, Coherent, operated at 30 μW), and a 532 nm Nd:YAG laser (Samba, Cobolt, operated at 240 μW), which were alternated at 20 kHz for single-molecule FRET measurements and which were operated in green continuous wave-mode for FCS measurements. The laser light was coupled into a 60×, 1.35 NA, UPlanSApo oil immersion objective (Olympus) and fluorescence signal from diffusing molecules was collected by the same objective and spectrally separated by a dichroic mirror (630DRLP, Omega) and directed on two avalanche photodiodes (SPCM-AQR14, Perkin Elmer). Photon arrival times were recorded with a PC counting National Instrument board and data processing was done using custom-written LabVIEW software (National Instruments). For *in vitro* confocal smFRET studies 20 μL of DNA FRET standards diluted in ddH_2O to 10–50 pM final concentration were added onto a burned cover slide and the laser beam was focused about 20 μm into solution; two 10 min data sets were acquired for each sample. The single-molecule fluorescence bursts from *in vitro* single-molecule FRET confocal microscopy were analysed in MATLAB as described in ref. 23 and as briefly described in the ESI.† For FCS measurements 20 μL of DNA FRET standards diluted in ddH_2O to 1–5 nM final concentration and single-molecule bursts were recorded for 5 min per data set at 120 μW green continuous wave and separated into green and red fluorescence channel for detection. The autocorrelation analysis is described in the ESI.†

Electroporation was performed using ElectroMAX DH5α-E Competent Cells (Invitrogen). The cells were diluted 1 : 1 with ddH_2O and stored at −80 °C. For each electroporation experiment protected DNA FRET standards were added to a final concentration of 50 nM to 20 μL of electrocompetent cells. The cell suspension was added into a pre-chilled electroporation cuvette (1 mm gap, Bio-Rad) and exposed to the discharge of a high voltage electric field with initial amplitude of 14 kV cm^{-1} (MicroPulser, Bio-Rad). The cells were rapidly recovered in 500 μL of super optimal broth with catabolite repression (SOC) for about 20 min shaking at 37 °C. Then, the cells were washed 4 times with phosphate buffered saline (PBS) by pelleting the cells by centrifugation at 3300*g* for 1 min at 4 °C, followed by resuspension. Finally, the cells were resuspended in about 100 μL PBS and stored on ice. About 5–10 μL of the cell suspension were spread on 1% agarose-M9 pads. Finally, a burned cover slide was placed on top of the agarose pad and turned towards the immersion oil objective for imaging.

In vivo single-molecule FRET measurements were performed under HILO illumination[34] on a custom-built inverted widefield microscope.[23] Laser light from two lasers, a 637 nm diode laser (Vortran Stradus Laser Technology) and a 532 nm DPSS laser (MGL-III-532 nm-100 mW, CNI) operated in green continuous wave-mode at 100 W cm^{-2} green excitation or in ALEX-mode at 100 W cm^{-2} green excitation, and 50 W cm^{-2} red excitation, was focused onto the backfocal plane of the objective and cellular fluorescence was collected through the same oil-immersion objective (UPLSAPO, 100×, NA 1.4, Olympus) and spectrally separated by a dichroic mirror (630DRLP, Omega). Each channel was imaged onto separate halves of an EMCCD camera chip (iXon+, BI-887, Andor). The illumination for brightfield images comprised a white-light lamp (IX2-ILL100, Olympus), which was attached to the microscope body. Movies and images were recorded using Andor camera software. Single-molecule FRET movies were analyzed using custom-written MATLAB software. *In vivo* smFRET analysis is further described in the ESI.†

Acknowledgements

We thank Timothy Craggs and Antonio Garcia Guerra for helpful discussions. A. P. was supported by a UK EPSRC DTA studentship and the German National Academic Foundation (Studienstiftung). A. P. held the Phizackerley Senior Scholarship in the Medical Sciences at Balliol College, Oxford. A. N. K. was supported by a UK BBSRC grant (BB/H01795X/1), and a European Research Council Starter grant (ERC 261227). T. B., A. N. K. and A. H. E.-S. thank the UK BBSRC for funding *via* the sLOLA grant BB/J001694/1: "Extending the Boundaries of Nucleic Acid Chemistry".

Notes and references

1 S. J. Lord, H. L. Lee and W. E. Moerner, *Anal. Chem.*, 2010, **82**, 2192–2203.
2 X. S. Xie, P. J. Choi, G. W. Li, N. K. Lee and G. Lia, *Annu. Rev. Biophys.*, 2008, **37**, 417–444.
3 S. Weiss, *Science*, 1999, **283**, 1676–1683.
4 T. Ha, *Methods*, 2001, **25**, 78–86.
5 M. Sustarsic and A. N. Kapanidis, *Curr. Opin. Struct. Biol.*, 2015, **34**, 52–59.
6 T. Förster, *Ann. Phys.*, 1948, **437**, 55–75.
7 L. Stryer and R. P. Haugland, *Proc. Natl. Acad. Sci. U. S. A.*, 1967, **58**, 719–726.
8 T. Ha, T. Enderle, D. F. Ogletree, D. S. Chemla, P. R. Selvin and S. Weiss, *Proc. Natl. Acad. Sci. U. S. A.*, 1996, **93**, 6264–6268.
9 B. Schuler, E. A. Lipman and W. A. Eaton, *Nature*, 2002, **419**, 743–747.
10 R. Zhao and D. Rueda, *Methods*, 2009, **49**, 112–117.
11 T. D. Christian, L. J. Romano and D. Rueda, *Proc. Natl. Acad. Sci. U. S. A.*, 2009, **106**, 21109–21114.
12 Y. Santoso, C. M. Joyce, O. Potapova, L. Le Reste, J. Hohlbein, J. P. Torella, N. D. Grindley and A. N. Kapanidis, *Proc. Natl. Acad. Sci. U. S. A.*, 2010, **107**, 715–720.
13 A. N. Kapanidis, E. Margeat, S. O. Ho, E. Kortkhonjia, S. Weiss and R. H. Ebright, *Science*, 2006, **314**, 1144–1147.
14 S. Arslan, R. Khafizov, C. D. Thomas, Y. R. Chemla and T. Ha, *Science*, 2015, **348**, 344–347.
15 S. Liu, B. T. Harada, J. T. Miller, S. F. Le Grice and X. Zhuang, *Nat. Struct. Mol. Biol.*, 2010, **17**, 1453–1460.
16 A. Plochowietz and A. N. Kapanidis, *Nat. Methods*, 2015, **12**, 715–716.
17 N. C. Shaner, P. A. Steinbach and R. Y. Tsien, *Nat. Methods*, 2005, **2**, 905–909.
18 T. Ha and P. Tinnefeld, *Annu. Rev. Phys. Chem.*, 2012, **63**, 595–617.
19 S. A. Jones, S. H. Shim, J. He and X. Zhuang, *Nat. Methods*, 2011, **8**, 499–508.
20 A. Keppler, S. Gendreizig, T. Gronemeyer, H. Pick, H. Vogel and K. Johnsson, *Nat. Biotechnol.*, 2003, **21**, 86–89.
21 R. Wombacher, M. Heidbreder, S. van de Linde, M. P. Sheetz, M. Heilemann, V. W. Cornish and M. Sauer, *Nat. Methods*, 2010, **7**, 717–719.
22 C. C. Liu and P. G. Schultz, *Annu. Rev. Biochem.*, 2010, **79**, 413–444.
23 R. Crawford, J. P. Torella, L. Aigrain, A. Plochowietz, K. Gryte, S. Uphoff and A. N. Kapanidis, *Biophys. J.*, 2013, **105**, 2439–2450.
24 J. J. Sakon and K. R. Weninger, *Nat. Methods*, 2010, **7**, 203–205.
25 I. Konig, A. Zarrine-Afsar, M. Aznauryan, A. Soranno, B. Wunderlich, F. Dingfelder, J. C. Stuber, A. Pluckthun, D. Nettels and B. Schuler, *Nat. Methods*, 2015, **12**, 773–779.
26 M. Sustarsic, A. Plochowietz, L. Aigrain, Y. Yuzenkova, N. Zenkin and A. Kapanidis, *Histochem. Cell Biol.*, 2014, **142**, 113–124.
27 A. Plochowietz, R. Crawford and A. N. Kapanidis, *Phys. Chem. Chem. Phys.*, 2014, **16**, 12688–12694.
28 E. Friedberg, *DNA Repair and Mutagenesis*, American Society of Microbiology, 2006.
29 E. T. Kool, *Annu. Rev. Biophys. Biomol. Struct.*, 1996, **25**, 1–28.
30 I. K. Lee, J. D. Ahn, H. S. Kim, J. Y. Park and K. U. Lee, *Curr. Drug Targets*, 2003, **4**, 619–623.
31 A. N. Kapanidis, N. K. Lee, T. A. Laurence, S. Doose, E. Margeat and S. Weiss, *Proc. Natl. Acad. Sci. U. S. A.*, 2004, **101**, 8936–8941.
32 N. K. Lee, A. N. Kapanidis, Y. Wang, X. Michalet, J. Mukhopadhyay, R. H. Ebright and S. Weiss, *Biophys. J.*, 2005, **88**, 2939–2953.
33 S. A. Kooijmans, S. Stremersch, K. Braeckmans, S. C. de Smedt, A. Hendrix, M. J. Wood, R. M. Schiffelers, K. Raemdonck and P. Vader, *J. Controlled Release*, 2013, **172**, 229–238.
34 M. Tokunaga, N. Imamoto and K. Sakata-Sogawa, *Nat. Methods*, 2008, **5**, 159–161.
35 S. J. Holden, S. Uphoff and A. N. Kapanidis, *Nat. Methods*, 2011, **8**, 279–280.
36 J. Hohlbein, L. Aigrain, T. D. Craggs, O. Bermek, O. Potapova, P. Shoolizadeh, N. D. Grindley, C. M. Joyce and A. N. Kapanidis, *Nat. Commun.*, 2013, **4**, 2131.

